

Synthesis of Chitin-Ionic Liquid Beads as Potential Adsorbents for Methylene Blue

Nor Shahirah Abdul Hamid¹, Faizah Naseeruteen¹, Wan Saime Wan Ngah¹, Noor Fadilah Yusof², Faizatul Shimal Mehamod² and Faiz Bukhari Mohd Suah^{1*}

¹School of Chemical Sciences, Universiti Sains Malaysia, 11800 Minden, Pulau Pinang, Malaysia.

²School of Fundamental Science, Universiti Malaysia Terengganu, 21030 Kuala Nerus, Malaysia.

*Corresponding author (e-mail: fsuah@usm.my)

The adsorption of methylene blue (MB) by chitin-ionic liquid beads was carried out with three different types of ionic liquids (ILs); 1-butyl-3-methyl imidazolium acetate (BMIM Ac), 1-butyl-3-methyl imidazolium chloride (BMIM Cl), and 1-allyl-3-methyl imidazolium bromide (AMIM Br). These three ILs were used to investigate the compatibility with chitin in forming adsorbates for MB adsorption. Batch adsorption experiments were conducted to investigate the optimum parameters such as pH, MB initial concentrations, adsorbent dosage, and contact time for adsorption of MB. The kinetic study revealed that pseudo-second order was the appropriate kinetic model for all the synthesized chitin-ILs, whereas Langmuir isotherm gave the best isotherm model for describing the adsorption mechanism of the chitin-ILs towards MB. The calculated q_{max} for the chitin powder, chitin-BMIM Ac beads, chitin-BMIM Cl beads, and chitin-AMIM Br beads were 22.37 mg g⁻¹, 19.81 mg g⁻¹, 18.80 mg g⁻¹, and 13.79 mg g⁻¹, respectively.

Key words: Chitin beads; ionic liquids: methylene blue; 1-butyl-3-methyl imidazolium acetate; 1-butyl-3-methyl imidazolium chloride; 1-allyl-3-methyl imidazolium bromide

Received: July 2019; Accepted: May 2020

Color pollution, especially in wastewater disposed of by an array of industries, such as textile, paper production, paint industry, and pharmaceutical, not only gives bad visibility but also invites harmful effects towards aquatic life. The discharge of highly colored species such as synthetic dyes in industries brings toxicity and carcinogenic effects on living beings. Therefore, dyestuff wastewater has been the serious issue to be addressed in the field of wastewater treatment. Even at very small concentrations (less than 1 mg L⁻¹ for some dyes), dyes may exert undesirable effects on humans and ecosystems [1]. Accidental or long-term exposure to dyes can cause respiratory problems due to the inhalation of dyes [2]. In addition, skin irritation, watery eyes, sneezing, symptoms of asthma, and cancer can develop due to prolonged exposure to dyes [1].

Most dyes are of synthetic origins and have complex molecular structures, which make them very stable and difficult to biodegrade [2]. This poses a serious hazard to aquatic organisms. One of the famous dyes used in industries is methylene blue (MB). MB is a cationic dye with a chemical formula of C₁₆H₁₈ClN₃S. MB can be categorized as a heterocyclic aromatic compound, which at room temperature the physical properties of MB are solid, odorless, dark green beads, and when dissolved in water it produces a blue solution.

Numerous studies have been reported in literatures for various methods and applications in MB

removal, such as adsorption on sand [3], a variety of activated carbon compounds [4, 5], electrocoagulation [6, 7], ion exchange, and biological methods [8, 9]. These methods have been proved to be considerable methods for wastewater treatment but some improvements in the existing methods are desirable. These methods have low removal percentage characteristics, reduced efficiency, operational complex, and most importantly high cost of operation [3-10]. Other than the methods mentioned, removal of MB by ionic liquids (ILs) is one of the alternative ways to improve any drawbacks of existing methods [10, 11]. Their remarkable properties, such as high thermal and chemical stabilities, non-volatile, and high electrical conductivity have made them good adsorbent materials for a variety of desired molecules [12].

Recently, the interest of utilizing ILs as solvents to bioadsorbents has been reported [11]. The key advantage of bioadsorbents prepared from ILs is they could be customized to enhance chemical and physical properties depending on the needs [13-16]. ILs are able to dissolve bioadsorbents that are connected by intermolecular hydrogen bonds. These hydrogen bonds within chitosan chains are replaced by anions from the ILs thus contribute to dissolution of bioadsorbents. In addition, cations from ILs also form covalent bonds with reducing ends of chitosan. ILs are able to direct the split of the chitosan chains by the synergistic effects of anions and cations. This will contribute to the ring opening reaction, thus leading to a formation of covalent bonds between IL core and

chitosan. It was reported that bioadsorbents prepared from ILs exhibited better properties compared to bioadsorbents prepared from conventional solvents [14, 16]. Properties such as high stability, increased thermal stability, reduced thermal degradation, and improved separation (adsorption) capabilities were some of the properties yielded by bioadsorbents prepared from ILs [15]. Chitin is the second most abundant natural polysaccharides on Earth [13]. It can be found in microorganisms, algae, crustaceans, or insects. The most essential sources of chitin are fishery wastes, especially skeletons of crabs, shrimps, and lobsters or prawns. Chitin is low in toxicity, biodegradable, antibacterial, hydrophilic, and has good affinity for proteins. Due to these good properties, chitin is commonly used in many industries such as agricultural, food, and pharmaceutical. This polymer is also known to be an effective adsorbent in the adsorption of reactive dyes. For that reason, chitin has the potential to be a low-cost and effective adsorbent for reactive dye wastewater removal [14]. Further applications of chitin, such as an adsorbent or for enzyme immobilization, require modifications of its particles in order to increase its porosity, solubility, and surface area.

The present study demonstrated three types of ILs: 1-butyl-3-methylimidazolium acetate (BMIM Ac), 1-butyl-3-methylimidazolium chloride (BMIM Cl), and 1-allyl-3-methylimidazolium bromide (AMIM Br), combined with chitin beads used as potential adsorbents for MB removal from an aqueous solution. These ILs were chosen due to their ability to dissolve or swell chitin [12]. One of the ILs, BMIM Cl could dissolve cellulose in relatively high concentrations but there are few studies concerning the dissolution of chitin in ILs. Recently, it was found that all of the ILs used in this study could dissolve or swell chitin to form a weak gel [12-14].

The objective of this study was to study the potential application of chitin-IL beads as alternative adsorbents for an efficient treatment or recovery of MB. The uptake of MB on chitin-IL beads was investigated for their optimum conditions, such as pH, initial MB concentration, adsorbent dosage, and time taken. Adsorption isotherms and kinetic parameters were calculated and discussed further. Our previous study utilizing chitosan-IL beads in adsorption of malachite green from aqueous solutions showed very promising results [15]. Therefore, we have extended our investigation by employing another set of ILs as the chitin-IL beads for adsorption of MB.

CHEMICALS AND METHODOLOGIES

Chemicals

Chitin ((C₈H₁₃O₅N)_n) powder, 1-butyl-3-methylimidazolium acetate (C₁₀H₁₈N₂O₂), sodium hydroxide (NaOH) pellets, 37.0% hydrochloric acid (HCl), and acetic acid (CH₃COOH) were purchased from Sigma-Aldrich (Malaysia). 1-butyl-3-methylimidazolium

chloride (C₈H₁₅ClN₂) and 1-allyl-3-methylimidazolium bromide (C₇H₁₁BrN₂) were purchased from Merck (Malaysia). Methylene blue dye was purchased from R&M Chemicals (Malaysia). All the chemicals and reagents used in this study were of analytical grade and used without any purification process.

Preparation of Chitin-Ionic Liquid Beads

Chitin-BMIM Ac beads were prepared by mixing 7.5 mL of BMIM Ac and 0.75 g of chitin powder in a 1000 mL beaker. This mixture was heated and stirred at 110°C for 5 hours on a magnetic stirrer heater (Cimarec Barnsted Thermolyne Heater and Stirrer). A viscous solution was obtained after 5 hours, and 500 mL of 1 M sodium hydroxide (NaOH) was added to the viscous solution and the mixture was left stirring for another 2 hours without any heat supply. The beads obtained were then filtered and washed with a large amount of distilled water, and left to air-dry. The dried beads were then ground and sieved using a sieve (Retsch GmbH) to obtain uniform bead size of <300 μm. Similar procedures were used to prepare chitin-BMIM Cl and chitin-AMIM Br beads.

Characterization of Chitin-Ionic Liquid Beads

The surface and morphological properties of chitin, chitin-BMIM Ac, chitin-BMIM Cl, and chitin-AMIM Br beads were characterized using Scanning Electron Microscopy (SEM) model LEO Supra 50 VP. The chemical compositions of MB, chitin beads, and chitin-IL beads before and after MB adsorption were determined by Fourier Transformed Infrared (FTIR) with Perkin-Elmer 2000 Model spectrometer in a range of 4000–650 cm⁻¹ using Universal ATR sampling technique.

Batch Adsorption Experiment

Equilibrium batch rebinding experiments were carried out to determine the optimum pH, the effect of initial concentration of MB, the effect of chitin-IL dosage, and the effect of contact time. In determination of optimum pH, a set of MB solutions (10 mg L⁻¹) was prepared for pH range tested (pH 2–8). The pH of MB solutions was adjusted by adding HCl and NaOH. The absorbance of 20 mL of MB solution before adding 0.01 g of chitin-BMIM Ac, chitin-BMIM Cl, and chitin-AMIM Br beads was determined. The mixtures were agitated for a period of 60 min at 300 rpm.

The experimental effect of initial MB concentration was studied by preparing solutions with different concentrations of 5, 10, 15, and 20 mg L⁻¹. The solutions were adjusted to the optimum pH obtained in the equilibrium batch rebinding experiment by adding HCl or NaOH. This study was done by using 0.01 g of adsorbent in 20 mL of MB solutions. The mixtures were agitated for 60 min at 300 rpm.

For the effect of adsorbent dosage, the chitin and three chitin-IL bead dosages were varied from 0.002 to 0.01 g while other parameters were kept constant. The experiments were conducted at room temperature using 20 mL of the optimum concentrations of MB solutions which were 20 mg L⁻¹ for chitin beads, chitin-BMIM Ac beads, and chitin-BMIM Cl beads, and 10 mg L⁻¹ for chitin-AMIM Br beads (and adjusted to optimum pH). The mixtures were agitated for 60 min at 300 rpm.

For the effect of contact time, 5 sets of 20 mL mixture of MB solution containing 0.01 g of adsorbent at optimum pH and optimum concentrations of the chitin and three chitin-IL beads were prepared. The optimum contact time was investigated by varying the agitation time at 10, 20, 30, 40, and 50 min at stirring speed of 300 rpm.

After the adsorption process was completed for all parts of the experiment (continuous method for each part), the filtered solutions were analyzed by Perkin-Elmer Lambda 35 Ultraviolet-Visible spectrophotometer at 663 nm, which is the absorption wavelength of MB. Two additional replicate analyses were conducted to enhance the accuracy of the data. The uptake capacity (mg g⁻¹) or the amount of MB adsorbed on the chitin-IL beads at equilibrium (q_e) and the percentage removal of MB (%R) were calculated by using Eq. 1 and Eq. 2, respectively:

$$q_e = \frac{(C_o - C_e)}{m} \times V \quad (1)$$

$$\%R = \frac{(C_o - C_e)}{C_o} \times 100\% \quad (2)$$

where C_o is the initial concentration of MB (mg L⁻¹), C_e is the concentration of MB at equilibrium (mg L⁻¹), V is the volume of MB (L), and m is the weight of the beads (g).

RESULTS AND DISCUSSION

1. Characterization of Chitin-IL Beads

1.1. Scanning Electron Microscopy

The surface morphology of the prepared beads is shown in Figure 1. As is obvious in the micrographs, there were remarkable differences seen in the morphology properties between each chitin-IL before and after modification with ILs. The surfaces of the chitin-ILs were very rough and irregular. There were also holes and small openings on the surface of the chitin-IL beads and this result was similar to our previous study, which was on the modification of chitosan-ILs [15]. It was expected that the holes and openings of the chitin-IL beads would increase the contact area, which facilitated pore diffusion during the adsorption process.

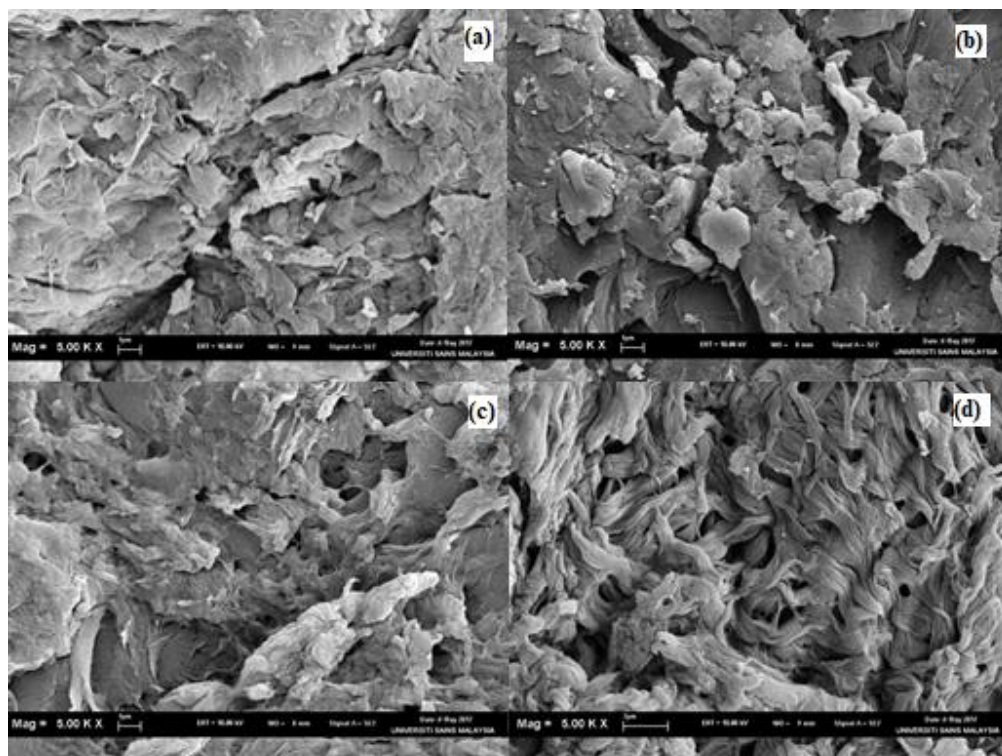
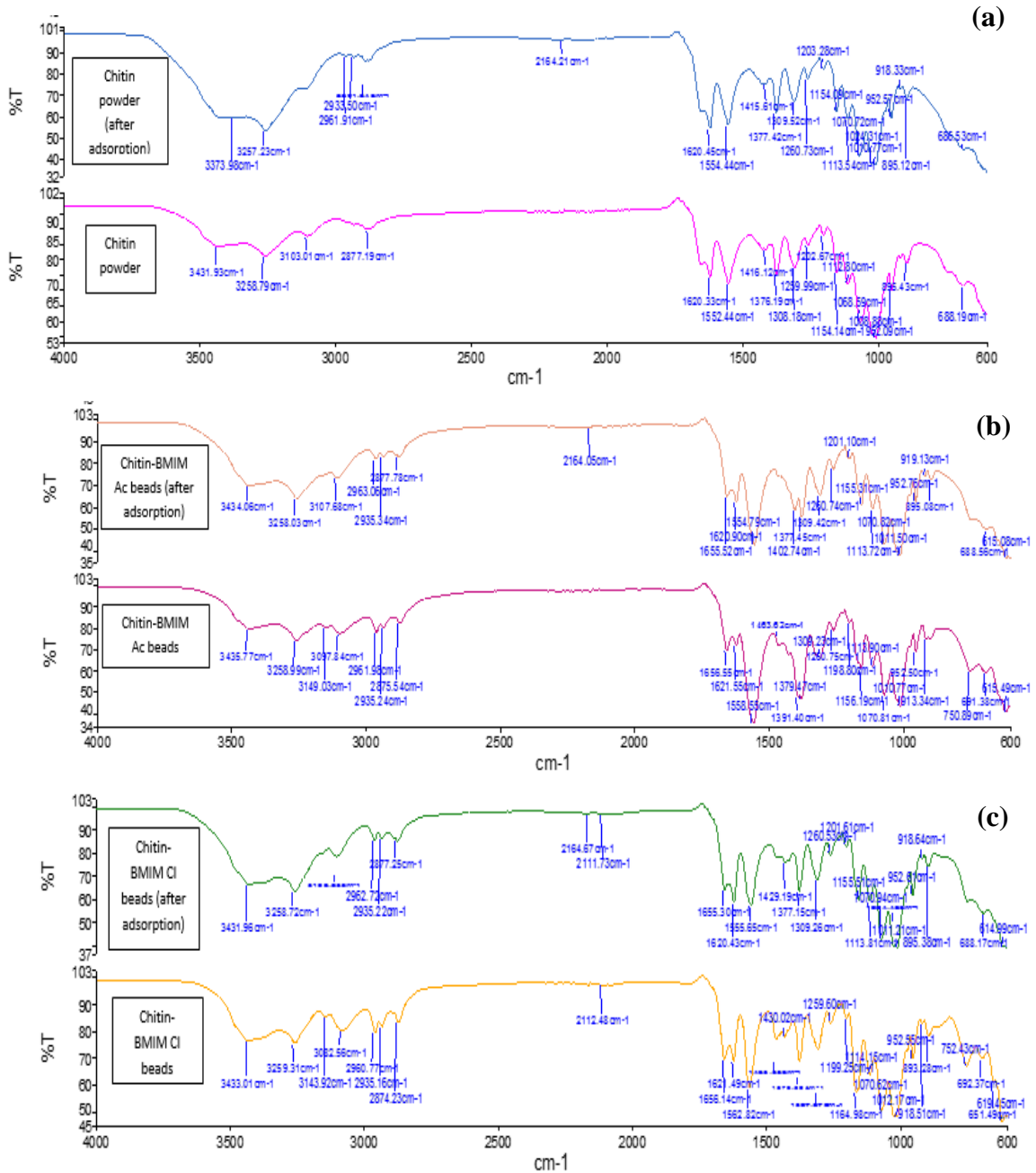


Figure 1. SEM micrographs for (a) chitin, (b) chitin-BMIM Ac, (c) chitin-BMIM Cl, and (d) chitin-AMIM Br beads at 5000× magnification.

Table 1. Physical properties of chitin and chitin-ILs beads.

Properties/ Adsorbent	Chitin beads	Chitin-BMIM Ac beads	Chitin-BMIM Cl beads	Chitin-AMIM Br beads
BET Surface Area (m ² g)	4.304	2.401	6.952	2.756
Langmuir Surface Area (m ² g)	5.143	6.159	9.929	4.129
Average pore diameter (Å)	10.226	18.171	25.521	15.666



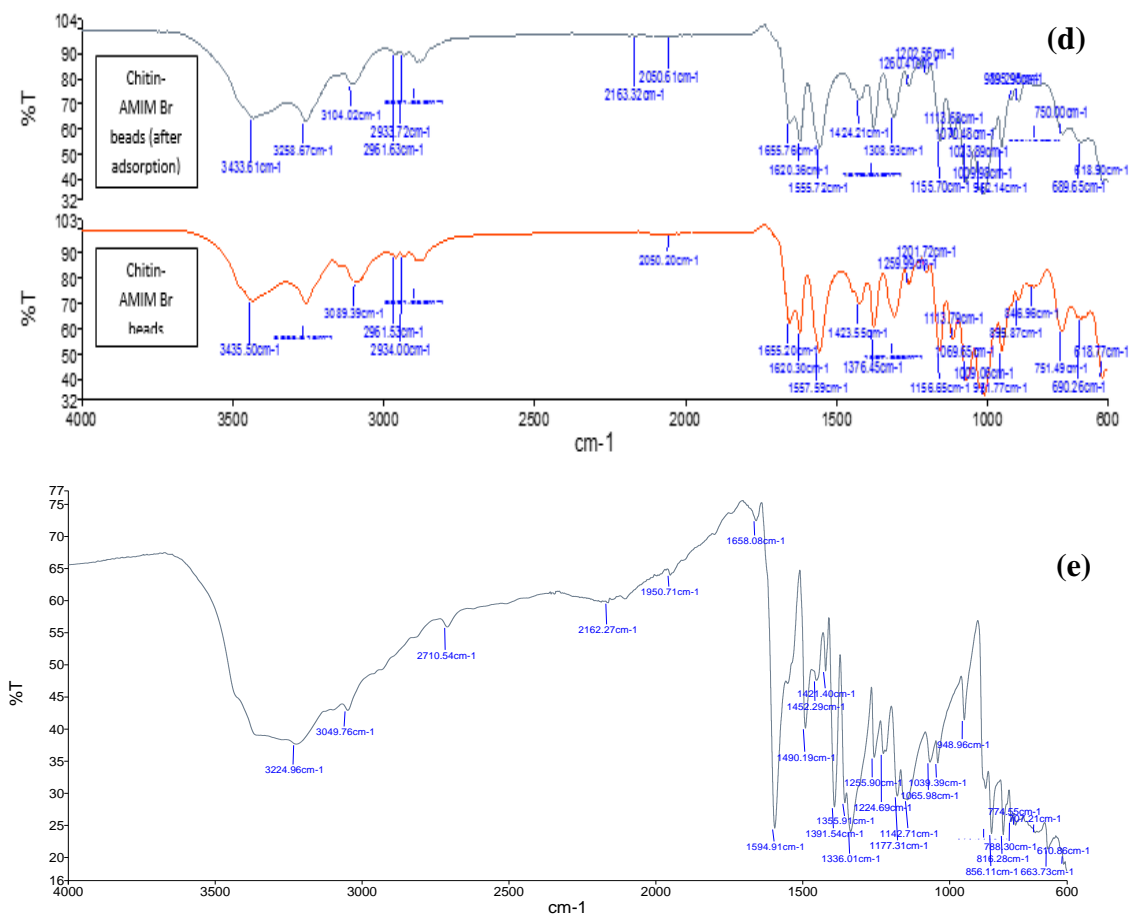


Figure 2. FTIR spectra of (a) chitin beads before and after adsorption, (b) chitin-BMIM Ac beads before and after adsorption, (c) chitin-BMIM Cl beads before and after adsorption, (d) chitin-AMIM Br beads before and after adsorption, and (e) MB.

1.2. Surface Area, Pore Volume, and Pore Size

Nitrogen adsorption-desorption analysis was carried out to determine the surface area, pore volume, and pore size of the chitin and synthesized chitin-IL beads. The Brunauer-Emmett-Teller (BET) theory was used to determine the specific surface area based on multilayer adsorption and Langmuir surface area based on monolayer adsorption.

summarizes the values of BET surface area and average pore diameter obtained for pure chitin and chitin-IL beads. Chitin-BMIM Cl beads had the highest surface area compared to pure chitin beads. This could be due to the presence of numerous pores developed on the surface. It was also noted that pore diameters of all the chitin-IL beads increased as compared to the pure chitin beads. These pores developed due to the solubility effect of ILs utilized in this study. High solubility of solvents or ILs contributed to the increase of pore size and surface area. Both cations and anions in ILs used in this study were responsible for this observation, especially the cations [13]. The highest solubility of chitin was obtained for BMIM Cl, followed by BMIM Ac and finally AMIM Br-based ILs [17]. ILs high solubility

was able to modify the surface of chitin beads by increasing their pore size. It was also interesting to observe that chitin-BMIM Ac beads and chitin-AMIM Br beads had lower surface area than the pure chitin beads. This could be explained by the size of the anions for each IL used [13]. Ac has ionic radius of 162 pm and Br has ionic radius of 196 pm [16]. Here, the small size of anions affected the physical size of the chitin beads which limited the expansion of the surface area. This observation confirmed that ILs were able to modify the physical properties of chitin beads. In addition, the average pore diameters for the chitin and chitin-IL beads were categorized as mesopores [16].

1.3. Structural Characterization by FTIR

The prepared chitin-IL beads were characterized by FTIR. Figure 2(a) to 2(d) show the FTIR spectra of chitin, chitin-BMIM Ac, chitin-BMIM Cl, and chitin-AMIM Br beads, respectively. Meanwhile, the FTIR spectrum of MB is shown in Figure 2(e). The bands at 3431 and 3258 cm⁻¹ were attributed to the OH and NH stretching, respectively. The shape and intensity of these peaks would change if the hydrogen

bonding network in chitin was altered. The bands ranging from 2877 to 3103 cm^{-1} represent CH, CH_3 symmetric stretching, and CH_2 asymmetric stretching. Meanwhile, the CH bending, symmetric CH_3 deformation, and CH_2 wagging bands appeared at 1376 and 1308 cm^{-1} . The peaks at $\sim 1620 \text{ cm}^{-1}$ were assigned to the Amide I band (two types of hydrogen bonds in a C=O group with the NH group of the adjacent chain and the OH group of the inter-chain). The Amide II band (in-plane N-H bending and C-N stretching mode) and Amide III band (in-plane mode of the CONH group) were observed at 1552 and 1416 cm^{-1} , respectively. The bands ranging from 1068 to 1154 cm^{-1} were attributed to the asymmetric bridge oxygen and C-O stretching [12]. Most of the peaks were comparatively similar to the spectra obtained for chitin beads.

For FTIR spectrum of MB, the peak at 3224.96 cm^{-1} was attributed to the N-H stretching, while the band at 3049 cm^{-1} represented C=C-H. The bands at 2710, 1950, and 1658.08 cm^{-1} showed the C-H stretch, C=N, and C=C stretch, respectively [14]. By comparing the spectra of the different chitin-IL beads, there were no new absorption bands found after MB adsorption. This suggested that the adsorption process did not involve chemical interaction, but a physical adsorption process had taken place [16].

2. Adsorption Studies

2.1. Effects of Initial pH

The influence of initial pH towards the adsorption

of MB was plotted (Figure 3). Based on the plot, the adsorption capacity (q_e) values for chitin and chitin-BMIM Cl beads increased with increase in pH value. For chitin-BMIM Ac beads, the q_e decreased after pH 4, whereas for chitin-AMIM Br beads, the q_e value showed a sudden drop at pH 6 that continued at pH 8. It could be concluded that for chitin and chitin-BMIM Cl beads the optimum pH was at pH 8, whereas for chitin-BMIM Ac and chitin-AMIM Br beads was at pH 4. The interaction between adsorbent (e.g. chitin-ionic liquid beads) and MB is affected by the pH of an aqueous medium because dyes are complex aromatic organic compounds having different functional groups and unsaturated bonds. They have different ionization abilities at different pH, resulting in the pH-dependent net charge on dye molecules [18].

2.2. Effects of Initial Concentration of MB

To study the influence of the initial concentration of MB, solutions were prepared in varying concentrations from 5 to 20 mg L^{-1} . Based on Figure 4, the higher the initial concentration of MB, the higher the q_e value. From the results obtained in this study, the concentration of 20 mg L^{-1} for all the beads indicated that the higher initial concentration provided an important driving force to overcome all the resistance of the dye between the aqueous and solid phases, thus increasing the uptake [19]. In addition, increasing the initial concentration of the dye would increase the number of collisions between the dye and beads, which finally enhanced the adsorption amount [20].

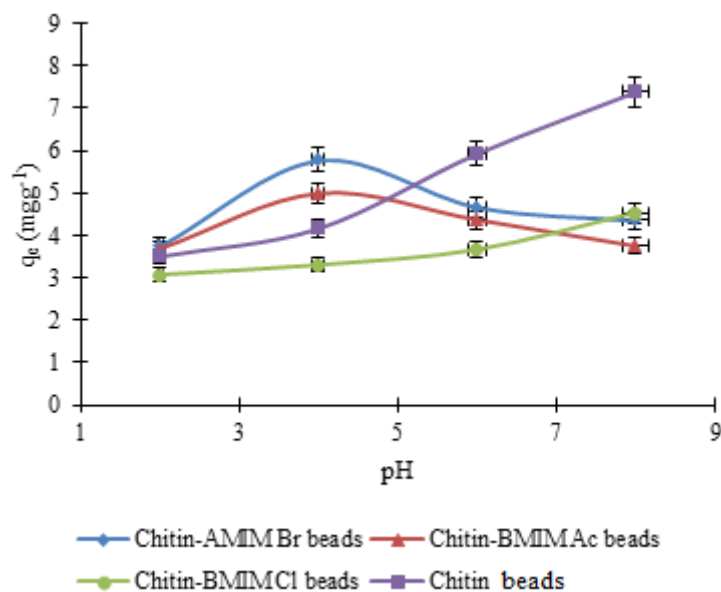


Figure 3. Effects of pH on the adsorption of MB dye onto different chitin beads.

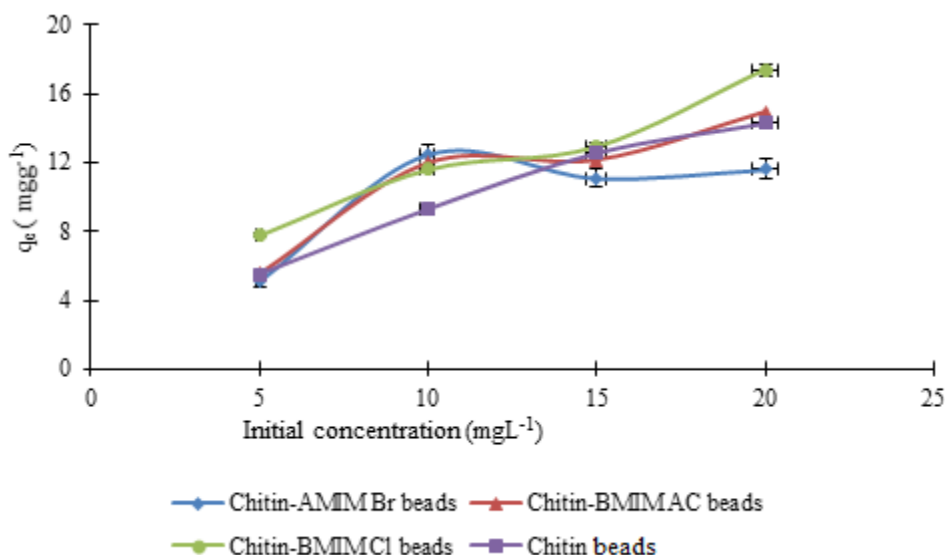


Figure 4. Effects of different initial concentration for the adsorption of MB onto different chitin beads.

2.3. Effects of Contact Time

Time is an important parameter in the binding study as it requires time for the adsorption of MB to reach an equilibrium state. The color of all four chitin-IL beads changed from pale white to light blue after the adsorption of MB. Figure 5 shows the effects of contact time for the adsorption of MB by different chitin beads. The adsorption was divided into two phases: an initial rapid phase and a second slower phase. The initial rapid phase occurred during the first 10 min of adsorption whereby the adsorption was fast due to the abundance of adsorption sites for the uptake

of MB. From the graphs plotted, the optimum agitation period for the chitin-IL beads was 20 min. For all of the beads, the adsorption increased from 0 and reached the highest adsorption at 20 min. After 20 min, equilibrium was reached due to exhaustion of the adsorption sites. The change in the rate of adsorption might be because initially all the adsorbent sites were vacant and the solute concentration gradient was very high. Later, the lower adsorption rate was due to the decrease in the number of vacant sites of the adsorbent and the dye concentration. This could be attributed to the lack of available active sites required for further uptake after attaining the equilibrium [21].

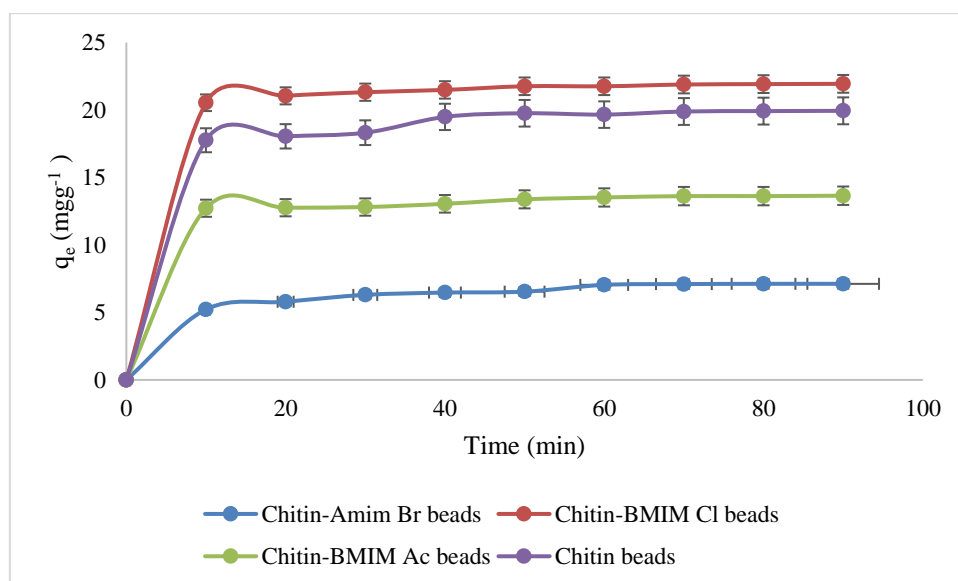


Figure 5. Effects of contact time on the adsorption of MB onto different chitin beads.

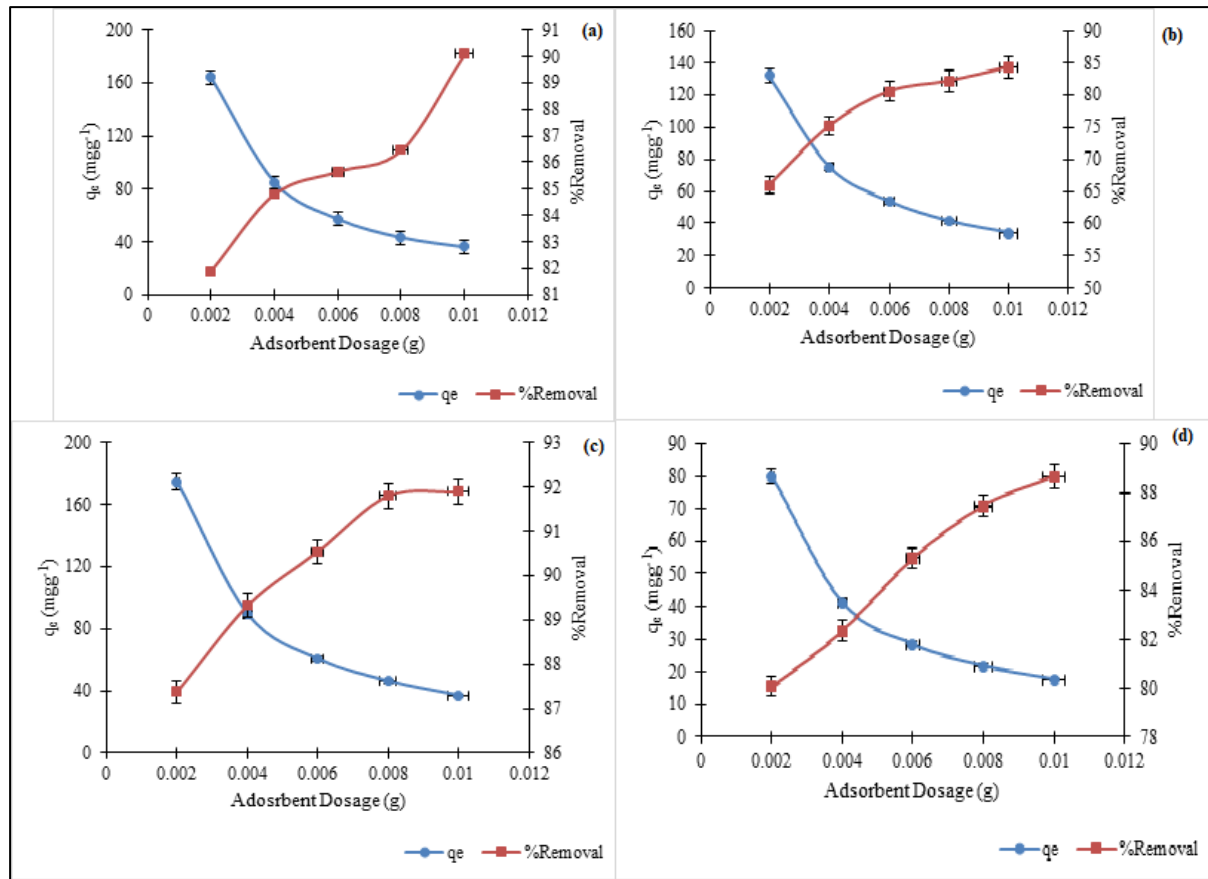


Figure 6. Effects of adsorbent dosage on the adsorption of MB onto (a) chitin, (b) chitin-BMIM Ac, (c) chitin-BMIM Cl, and (d) chitin-AMIM Br beads.

2.4. Effects of Adsorbent Dosage

The optimum dosage was determined by varying the amount of adsorbent mass of chitin-ILs. The effects of adsorbent dosage on the adsorption of MB onto different chitin-ILs are shown in Figure 6. It was observed that percentage removal recovers for all chitin-ILs increased steadily with the increase of adsorbent mass. This was mainly due to the increase of availability of active binding sites on the adsorbent surface. However, there was no equilibrium point for all samples except chitin-BMIM Cl beads, which showed the percentage removal had reached the optimum dosage at 0.008 g. It could be concluded that the changes in the quantity of adsorbent would have a direct effect on the binding of MB molecules when linear forms of isotherms were used [20, 21]. For the adsorption capacity, all the samples exhibited high q_e values at the mass of 0.002 g, which indicated all the adsorption sites were occupied by MB molecules as the first stage. Then, it was followed by steady decreases in q_e values as adsorbent dosage increased from 0.004 to 0.1 g.

2.5. Adsorption Isotherm Study

The equilibrium data obtained from the batch experiment were used to get information on the behaviour of the adsorption of MB onto the chitin-ILs. The Langmuir,

Freundlich, and Temkin isotherm models were used in this study and expressed mathematically as in Eq. 3, Eq. 4, and Eq. 5, respectively:

$$\frac{C_e}{q_e} = \frac{1}{Qb} + \frac{C_e}{Q}, \quad (3)$$

$$\log q_e = \log K_F + \frac{1}{n} \log C_e, \quad (4)$$

$$q_e = \frac{RT}{bT} \ln K_T + \frac{RT}{bT} \ln C_e, \quad (5)$$

where C_e is the equilibrium MB concentration (mg L⁻¹), q_e is adsorption capacity (mg g⁻¹), q_{max} is the maximum adsorption at monolayer (mg g⁻¹), b is the Langmuir constant related to the affinity of binding sites (L mg⁻¹) and the adsorption energy, K_F and $1/n$ are measures of the adsorption capacity (mg g⁻¹) and adsorption intensity, respectively, b_T is the Temkin constant related to the heat of adsorption (kJ mol⁻¹), K_T is the equilibrium binding constant corresponding to the maximum binding energy (L g⁻¹), T is the absolute temperature (K), and R is the gas constant (8.314 J K⁻¹ mol⁻¹).

The Langmuir isotherm model has four assumptions: (i) the forces of interaction between the adsorbed molecules are negligible, (ii) no further

adsorption occurs when the adsorption site is occupied, (iii) adsorption occurs at specific homogeneous adsorption sites within the adsorbent, and (iv) the intermolecular forces of attraction will be weakened rapidly with distance [3, 15, 22].

The graph of C_e/q_e versus C_e was plotted (Figure 7(a)). From the linear plot, the values of q_{max} and b could be calculated from the slope and the intercept, respectively. The values of q_{max} were almost the same as the experimental data (Table 2). A dimensionless constant separation factor, R_L was calculated to determine whether the Langmuir type adsorption process was favorable.

The shapes of the isotherms could be divided into favorable, unfavorable, linear and irreversible when $0 < R_L < 1$, $R_L > 1$, $R_L = 1$, and $R_L = 0$, respectively. R_L is expressed mathematically as follows [21]:

$$R_L = \frac{1}{1 + bC_o}, \quad (6)$$

where b is the Langmuir constant ($L \text{ mg}^{-1}$) and C_o is

the initial MB concentration (mg L^{-1}). The calculated R_L values are tabulated in Table 3. The values of R_L lied between 0 and 1, showing that favorable adsorption had taken place in the adsorption mechanism.

The Freundlich isotherm, on the other hand, assumes a heterogeneous adsorption surface with sites that have different energies of adsorption. The Freundlich isotherm is an empirical isotherm used for multilayer adsorption. The Freundlich constants, K_F and n were obtained from the plot of $\log q_e$ versus $\log C_e$ (Figure 7(b)). The higher the K_F value, the higher the maximum capacity. The n value is the most important parameter from the Freundlich equation. If the n value is larger than unity, it indicates that the bonds between the adsorbent and adsorbate are strong. Stronger bond will give a higher value of n . The value of n also indicates whether the adsorption process is favorable or not; if it is larger than unity, it is favorable. From Table 2, the n values were all larger than unity. This showed that the adsorption process was favorable.

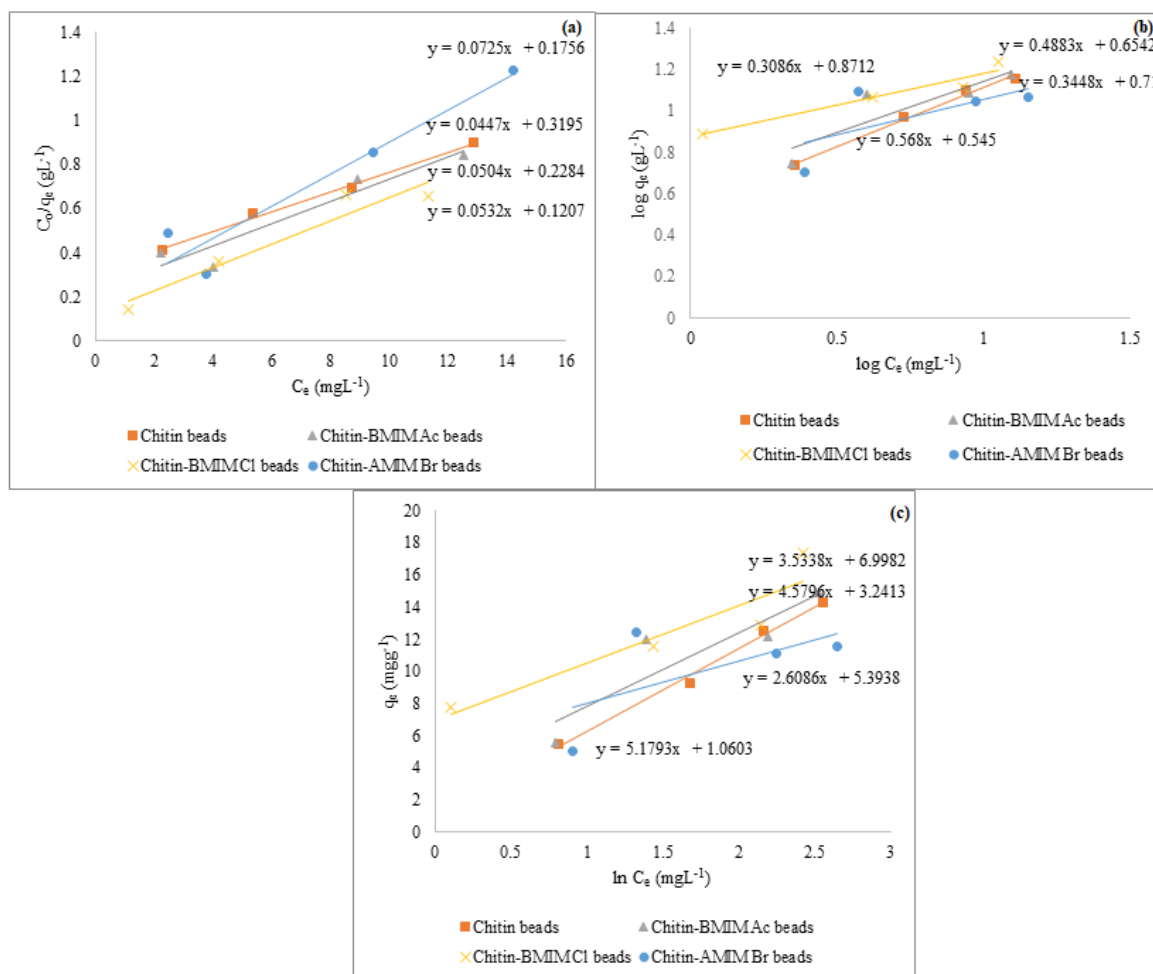


Figure 7. Plots of (a) Langmuir, (b) Freundlich, and (c) Temkin isotherms for adsorption of MB onto different chitin beads.

Table 2. Langmuir, Freundlich, and Temkin isotherm constants and correlations for the adsorption of MB onto different chitin-IL beads.

	Isotherm								
	Langmuir			Freundlich			Temkin		
	q_{max} (mg g ⁻¹)	b (Lmg ⁻¹)	R ²	K_F (mg g ⁻¹)	N	R ²	b_T (kJmol ⁻¹)	K_T (L g ⁻¹)	R ²
Chitin beads	22.372	0.140	0.995	0.545	1.761	0.991	478.360	1.227	0.993
Chitin-BMIM Ac beads	19.811	0.221	0.912	0.222	2.048	0.773	541.002	2.030	0.817
Chitin-BMIM Cl beads	18.801	0.441	0.924	0.135	3.240	0.933	701.107	1.980	0.863
Chitin-AMIM Br beads	13.791	0.413	0.921	0.195	2.900	0.435	949.771	2.068	0.390

Table 3. Values of R_L for initial concentration range from 5 to 20 mg L⁻¹.

Initial Concentration (mg L ⁻¹)	R_L					
	Chitin beads	Chitin- BMIM beads	Ac	Chitin-BMIM Cl beads	Chitin- AMIM beads	Br
5	0.589	0.475		0.312	0.326	
10	0.417	0.312		0.185	0.195	
15	0.323	0.232		0.131	0.139	
20	0.263	0.185		0.102	0.108	

The Temkin isotherm contains a factor that explicitly takes into account the adsorbing species-adsorbent interactions. This isotherm assumes that (i) the heat of adsorption of all molecules in the layer decreases linearly with coverage due to adsorbent-adsorbate interactions and that (ii) the adsorption is characterized by a uniform distribution of binding energies, up to some maximum binding energy [22, 23]. The Temkin constants, b_T and K_T were obtained from the plot of q_e versus $\ln C_e$ (Figure 7(c)). The value of the Temkin constant b_T was related to the heat of adsorption of MB, and a high value indicated a strong interaction between the adsorbate and adsorbent.

The summarized data for Langmuir, Freundlich and Temkin isotherm constants for the adsorption of MB onto the chitin-IL beads are tabulated in Table 2. A comparison of R² values obtained for the three isotherms was made and it was found that the Langmuir isotherm gave the highest correlation coefficient among the isotherm models, which were greater than 0.9. Therefore, it was clear that the Langmuir isotherm has the best fit for the experimental data of the adsorption of MB onto different chitin beads. This showed that the adsorption of MB onto different chitin beads was more of monolayer adsorption rather than adsorption on a surface having a heterogeneous energy distribution.

2.6. Kinetic Study

A kinetic model is important to determine the rate of adsorption of an adsorbate and the rate-determining step. The rate of adsorption and rate-determining step are crucial in any adsorption process, especially for designing an adsorption system of a full-scale batch process. Three types of kinetic models were tested; pseudo-first order (Eq. 7), pseudo-second order (Eq. 8), and intraparticle diffusion (Eq. 9) models, to fit the batch equilibrium data [22, 23]:

$$\log (q_e - q_t) = \log q_e - \frac{k_1 t}{2.303}, \quad (7)$$

$$\frac{t}{q_t} = \frac{1}{k_2 q_e^2} + \frac{t}{q_e}, \quad (8)$$

$$q_t = k_p t^{1/2} + C, \quad (9)$$

where: q_e and q_t (mg g⁻¹) are the amounts of MB adsorbed onto the chitin-IL beads at equilibrium and time t (min), respectively; k_1 (min⁻¹) and k_2 (g mg⁻¹ min⁻¹) are the rate constants of adsorption in pseudo-first order and pseudo-second order equations, respectively; k_p is the intraparticle diffusion rate constant (mg g⁻¹ min^{1/2}); and C is the intercept for the intraparticle diffusion model (mg g⁻¹).

The linearized graphs of all models (pseudo-first order, pseudo-second order, and intraparticle diffusion) were plotted as shown in Figure 8. The pseudo-first order kinetic model was based on the assumption that the adsorption rate was proportional to the number of free adsorption sites [24-26]. Compared with the pseudo-first order, the pseudo-second order was more likely to predict the behaviour over the whole range of the adsorption process [25]. This model also assumed that the rate-limiting step

might be due to physical adsorption process that had taken place [27-29]. The intraparticle diffusion model gave an idea of the rate-controlling step. The intercept, C obtained from the plot of q_t versus $t^{1/2}$ implied the boundary layer thickness. A larger value of C meant greater boundary layer effect. Because the straight-line plot did not pass through the origin ($C \neq 0$), it showed that there was some degree of boundary layer control but intraparticle diffusion was not the only rate-controlling step.

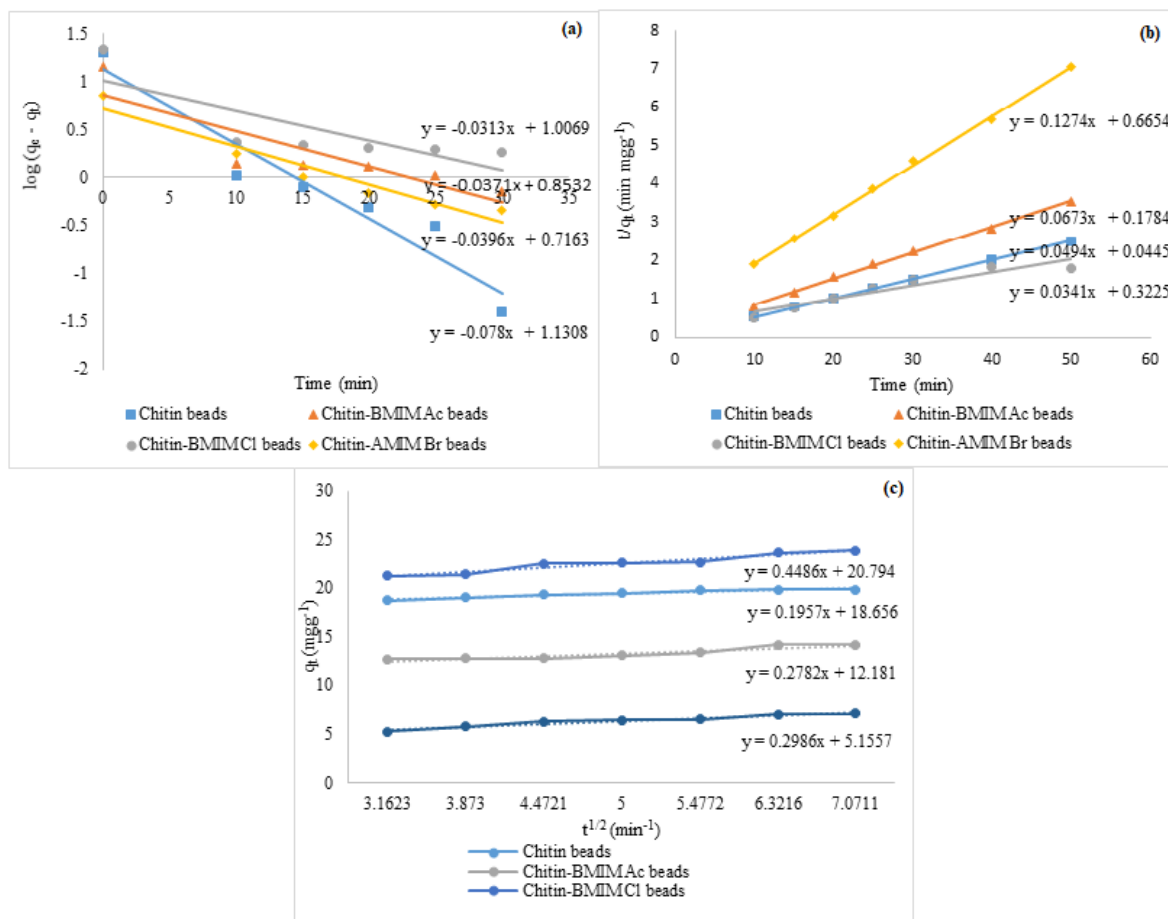


Figure 8. Plots of (a) pseudo-first order, (b) pseudo-second order, and (c) intraparticle diffusion for adsorption of MB on different chitin beads.

Table 4. Kinetics parameters for the adsorption of MB onto different chitin beads based on pseudo-first, pseudo-second, and intraparticle diffusion kinetic models.

	$q_{e,exp}$ (mg g^{-1})	Pseudo-First Order			Pseudo-Second Order			Intraparticle Diffusion		
		k_1 (min^{-1})	$q_{e,cal}$ (mg g^{-1})	R^2	k_2 (min g mg^{-1})	$q_{e,cal}$ (mg g^{-1})	R^2	k_p (mg $\text{g}^{-1} \text{in}^{1/2}$)	C (mg g^{-1})	R^2
Chitin beads	19.804	0.180	0.074	0.925	0.055	20.243	1.000	0.305	17.90	0.920
Chitin-BMIM Ac beads	14.142	0.086	0.140	0.758	0.026	14.859	0.997	0.444	11.05	0.888
Chitin-BMIM Cl beads	21.613	0.072	0.098	0.655	0.004	29.326	0.905	0.221	18.56	0.992
Chitin-AMIM Br beads	7.025	0.091	0.192	0.941	0.025	7.850	0.999	0.472	3.962	0.934

The kinetic parameters were calculated and tabulated in Table 4. Based on the results obtained, the adsorption of MB onto the chitin-IL beads was best described by the pseudo-second order model, as its coefficient of determination, R^2 was closest to 1 and the values of the calculated adsorption capacity ($q_{e,cal}$) and the experimental adsorption capacity ($q_{e,exp}$) were close to each other.

ACKNOWLEDGEMENTS

Authors would like to acknowledge Universiti Sains Malaysia for the financial assistance through short term research grant (304/PKIMIA/6313225). Two authors (F. Naseeruteen and N. S. A. Hamid) would like to thank Ministry of Education, Malaysia for granting their scholarships (MyBrain 15).

REFERENCES

1. Rafatullah, M., Sulaiman, O., Hashim, R. and Ahmad, A. (2010) Adsorption of methylene blue on low-cost adsorbents: a review, *Journal of Hazardous Materials*, **177**, 70–80.
2. Gupta, V. (2009) Application of low-cost adsorbents for dye removal—A review, *Journal of Environmental Management*, **90**, 2313–2342.
3. Bukallah, S. B., Rauf, M. A. and AlAli, S. S. (2007) Removal of methylene blue from aqueous solution by adsorption on sand, *Dyes and Pigments*, **74**, 85–87.
4. Pathania, D., Sharma, S. and Singh, P. (2017) Removal of methylene blue by adsorption onto activated carbon developed from *Ficus carica* bast, *Arabian Journal of Chemistry*, **10**, S1445–S1451.
5. Khodaie, M., Ghasemi, N., Moradi, B. and Rahimi, M. (2013) Removal of methylene blue from wastewater by adsorption onto $ZnCl_2$ activated corn husk carbon equilibrium studies, *Hindawi Journal of Chemistry*, Article ID 383985.
6. de Carvalho, H. P., Huang, J., Zhao, M., Liu, G., Dong, L. and Liu, X. (2015) Improvement of methylene blue removal by electrocoagulation/banana peel adsorption coupling in a batch system, *Alexandria Engineering Journal*, **54**, 777–786.
7. Mahmoud, M. S., Farah, J. Y. and Farrag, T. E. (2013) Enhanced removal of methylene blue by electrocoagulation using iron electrodes, *Egyptian Journal of Petroleum*, **22**, 211–216.
8. Cheng, M., Zeng, G., Huang, D., Lai, C., Wei, Z., Li, N., Xu, P., Zhang, C., Zhu, Y. and He, X. (2015) Combined biological removal of methylene blue from aqueous solutions using rice straw and *Phanerochaete chrysosporium*, *Applied Microbiology and Biotechnology*, **99**, 5247–5256.
9. Sonawane, G. H. and Shrivastava, V. S. (2009) Removal of basic dye (methylene blue) from aqueous solution by adsorption using *Musa paradisiaca*: a agricultural waste, *Journal of Environmental Science and Engineering*, **51**, 45–52.
10. Kermanioryani, M., Ismail, L. B., Mutalib, M. I. A. and Bagherzadeh, G. (2014) Removal of methylene blue from aqueous solution by ionic liquid, *Applied Mechanics and Materials*, **625**, 241–244.
11. Kermanioryani, M., Mutalib, M. I. A. Gonfa, G., El-Harbawi, M., Mazlan, F. A., Lethesh, K. C. and Leveque, J. M. (2016) Using tunability of ionic liquids to remove methylene blue from aqueous solution, *Journal of Environmental Chemical Engineering*, **4**, 2327–2332.
12. Kadokawa, J., Takegawa, A., Mine, S. and Prasad, K. (2011) Preparation of chitin nanowhiskers using an ionic liquid and their composite materials with poly(vinyl alcohol), *Carbohydrate Polymers*, **84**, 1408–1412.
13. Kadokawa, J. (2013) Ionic liquid as useful media for dissolution, derivatization and nanomaterial processing of chitin, *Green and Sustainable Chemistry*, **3**, 19–25.
14. Takegawa, A., Murakami, M., Kaneko, Y. and Kadokawa, J. (2010) Preparation of chitin/cellulose composite gels and films with ionic liquids, *Carbohydrate Polymers*, **79**, 85–90.
15. Naseeruteen, F., Abdul Hamid, N. S., Suah, F. B. M., Wan Ngah, W. S. and Mehamod, F. S. (2018) Adsorption of malachite green from aqueous solution by using novel chitosan ionic liquid beads, *International Journal of Biological Macromolecules*, **107**, 1270–1277.
16. Wang, W. T., Zhu, J., Wang, X. L., Huang, Y. and Wang, Y. Z. (2010) Dissolution behavior of chitin in ionic liquids, *Journal of Macromolecular Science, Part B*, **49**, 528–541.
17. Jaworska, M. M., Kozlecki, T. and Gorak, A. (2012) Review of the application of ionic liquids as solvents for chitin, *Journal of Polymer Engineering*, **32**, 67–69.
18. Aksu, Z., Ertuğrul, S. and Dönmez, G. (2009) Single and binary chromium(VI) and Remazol

- Black B biosorption properties of *Phormidium* sp, *Journal of Hazardous Materials*, **168**, 310–318.
19. Özer, A., Akkaya, G. and Turabik, M. (2006) The removal of Acid Red 274 from wastewater: combined biosorption and biocoagulation with *Spirogyra rhizopus*, *Dyes and Pigments*, **71**, 83–89.
 20. Cheng, W., Wang, S. G., Lu, L., Gong, W. X., Liu, X. W., Gao, B. Y. and Zhang, H. Y. (2008) Removal of malachite green (MG) from aqueous solutions by native and heat-treated anaerobic granular sludge, *Biochemical Engineering Journal*, **39**, 538–546.
 21. Yusoff, S. M., Wan Ngah, W. S., Mehamod, F. S. and Suah, F. B. M. (2019) Adsorption of malachite green onto modified chitosan-sulfuric acid beads: a preliminary study, *Malaysian Journal of Analytical Chemistry*, **23**, 625–636.
 22. Bekçi, Z., Özveri, C., Seki, Y. and Yurdakoç, K. (2008) Sorption of malachite green on chitosan bead, *Journal of Hazardous Materials*, **154**, 254–261.
 23. Choy, K. K. H., McKay, G. and Porter, J. F. (1999) Sorption of acid dyes from effluents using activated carbon, *Resources, Conservation and Recycling*, **27**, 57–71.
 24. Feizi, M. and Jalali, M. (2016) Sorption of aquatic phosphorus onto native and chemically-modified plant residues: modeling the isotherm and kinetics of sorption process, *Desalination and Water Treatment*, **57**, 3085–3097.
 25. Mustapha, S., Shuaib, D. T., Ndamitso, M. M., Sumaila, A., Mohammed, U. M. and Nasirudeen, M. B. (2019) Adsorption isotherm, kinetic and thermodynamic studies for the removal of Pb(II), Cd(II), Zn(II) and Cu(II) ions from aqueous solutions using *Albizia lebbek* pods, *Applied Water Science*, **9**, 142–153.
 26. Ngah, W. S. W. and Fatinathan, S. (2008) Adsorption of Cu(II) ions in aqueous solution using chitosan beads, chitosan–GLA beads and chitosan–alginate beads, *Chemical Engineering Journal*, **143**, 62–72.
 27. Ho, Y. S. and McKay, G. (1999) Pseudo-second order model for sorption processes, *Process Biochemistry*, **34**, 451–465.
 28. Akkaya, G., Uzun, I. and Guzel, F. (2007) Kinetics of the adsorption of reactive dyes by chitin, *Dyes and Pigments*, **73**, 168–177.
 29. Hameed, B. H. and Lee, T. W. (2009) Degradation of malachite green in aqueous solution by Fenton process, *Journal of Hazardous Materials*, **164**, 468–472.